

# SIX-PORT REFLECTOMETER BASED ON FOUR 0°/180° MICROSTRIP RING COUPLERS

Ashraf S. Mohra

Microstrip Department  
Electronics Research Institute  
National Research Center Building  
Tahrir Street, Dokki-Giza  
Cairo, Egypt

Received 27 June 2003

**ABSTRACT:** A six-port reflectometer constructed from a 0°/180° microstrip-ring coupler is presented. Three different constructions are given with their optimum positions of the  $q$ -point. One of these constructions is realized on an RT/Duroid 5880 at 3 GHz. Good agreement with the measurements obtained using a vector network analyzer is found. © 2004 Wiley Periodicals, Inc. *Microwave Opt Technol Lett* 40: 167–170, 2004; Published online in Wiley InterScience (www.interscience.wiley.com). DOI 10.1002/mop.11318

**Key words:** six-port reflectometer; microstrip ring coupler; calibration; reflection coefficient measurements

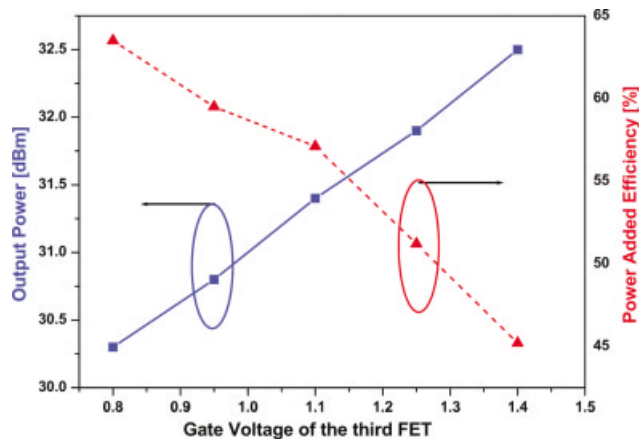


**Figure 10** PAE and output power as functions of gate-bias voltage [Color figure can be viewed in the online issue, which is available at www.interscience.wiley.com]

The PAE and output power of this PA module are measured as a function of the third-stage gate bias, as shown in Figure 10. From the figure, the output power increases as the gate-bias voltage increases, while the PAE decreases with an increasing gate bias.

## 5. CONCLUSION

In this paper, a modified level-3 technique has been presented for the nonlinear modeling of an RF LDMOS FET. This method takes advantage of a fast and easy modeling process. The design of the PA module uses the extracted parameters, which allows us to verify a large-signal analysis. The measurement results of the output power for the designed PA module are 30.3 dBm with PAE of 64% at 880 MHz.

The LDMOS PA module presented in this paper introduces techniques, such as HTN and WTN, to accomplish the proper optimization between output power and PAE.

## ACKNOWLEDGMENTS

This work has been partially supported by a research grant from Kwangwoon University in 2002 and by the Korean Ministry of Information and Communication through the ITRC project at RFIC Center.

## REFERENCES

1. W.R. Curtice, J.A. Pla, D. Bridges, T. Liang, and E.E. Shumate, A new dynamic electro-thermal nonlinear model for silicon RF LDMOS FETs, *IEEE MTT-S IMS Dig 2* (1999), 419–422.
2. F.M. Rotella, Modeling, analysis, and design of RF LDMOS devices using harmonic-balance device simulation, *IEEE Trans Microwave Theory Tech* 48 (2000), 991–999.
3. J.M. Collantes, J.J. Raoux, and R. Quere, New measurement-based technique for RF LDMOS nonlinear modeling, *IEEE Microwave Guided Wave Lett* 8 (1998), 345–347.
4. H. Fukui, Determination of the basic device parameters of GaAs MES-FET, *Bell Syst Tech J* (1979), 771–797.
5. S. Toyoda, High-efficiency amplifiers for 8-GHz band, *IEEE MTT-S IMS Dig 2* (1996), 689–692.
6. J.A.G. Slatter, An approach to the design of transistor tuned power amplifier, *IEEE Trans Circuit Theory* 12 (1965), 206–211.
7. M.K. Kazimierzczuk and W.A. Tabisz, Class C-E high efficiency tuned power amplifier, *IEEE Trans Circuit Syst* 36 (1989), 421–428.

© 2004 Wiley Periodicals, Inc.

## 1. INTRODUCTION

The six-port reflectometer, an inexpensive alternative to the network analyzer, is a simple device that does not need high-precision components and requires only power meters in order to measure complex impedances (see Fig. 1). The six-port reflectometer allows the phase and magnitude of an unknown complex impedance to be measured directly at the operating frequency (in terms of power measurement alone) by using a calibrating procedure. From the scalar measurements taken by the four power detectors, a circle in the  $\Gamma$ -plane is associated with each  $P_k/P_2$  ( $k = 1, 3, 4$ ) power ratio (see Fig. 2), and the solution is given by the (ideally) common intersection of the three circles derived from the measured data [1]. There are different methods to implement the six-port reflectometer, such as using two directional couplers and two voltage probes [2], and using three-coupled lines (coaxial lines, stripline, waveguide, or microstrip lines) [3, 4]. Another way is by using a five-port junction (ring or disc) and a directional coupler [5]. Many six-port reflectometers have been realized by using quadrature hybrids and directional couplers [6], but only a few use the 0°/180° ring coupler [7], where only a single construction and a single solution are described for the locations of the  $q$  points (center points of the circles that describe the power ratios).

In fact, some reflectometers utilizing the hybrid coupler yielded nonideal uniform distribution of the  $q$  points such that their locations were described as [7]:

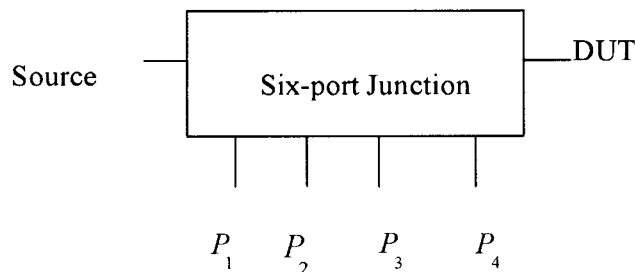


**Figure 1** Six-port reflectometer

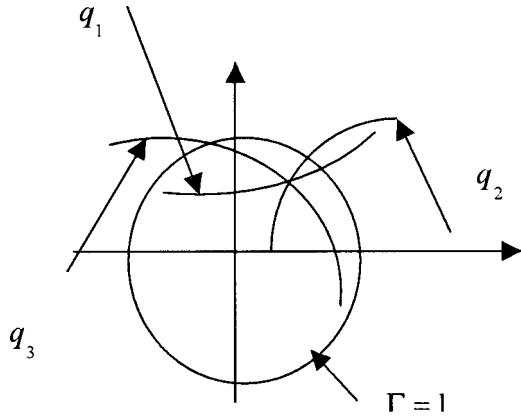


**Figure 2** Common intersection point in the complex  $\Gamma$ -Plane

- 90°, 90°, and 180° for the first generation of the six-port reflectometer proposed in [8];
- 90°, 135°, and 135° for reflectometer adopted in [9];
- 110°, 125°, and 125° for the improved design in [10]

In this paper, the analysis and design of the six-port reflectometer, which is constructed from four 0/180° microstrip ring couplers, are given. Three constructions for the six-port reflectometer are obtained with their different  $q$  points. As an example, the third construction was realized on an RT/Duroid 5880 at 3-GHz center frequency using a photolithographic technique and thin-film technology. The third construction's calibration and application for measuring different unknown impedances will be clarified in the following sections.

## 2. ANALYSIS

By using four conventional 0/180° couplers, as shown in Figure 3(a), the power equations related to the power-ratio reading of the six-port reflectometer will not achieve the required position of the  $q$  values. To overcome this problem, Eng et al. [7] suggest a solution that involves adding an electrical length  $\theta$  to only two arms of the four ring coupler [Fig. 3(b)], so that the  $S$  parameters of the modified ring coupler will take the following form:

$$S = \frac{-j}{\sqrt{2}} \begin{bmatrix} 0 & 0 & e^{-j\theta} & e^{-j2\theta} \\ 0 & 0 & -1 & e^{-j\theta} \\ e^{-j\theta} & -1 & 0 & 0 \\ e^{-j2\theta} & e^{-j\theta} & 0 & 0 \end{bmatrix}. \quad (1)$$

In fact, three constructions were made in order to realize the six-port reflectometer. Eng et al. [7] describe only one construction with only one solution. Here, we represent three constructions, each with two solutions. In all three constructions, we use four

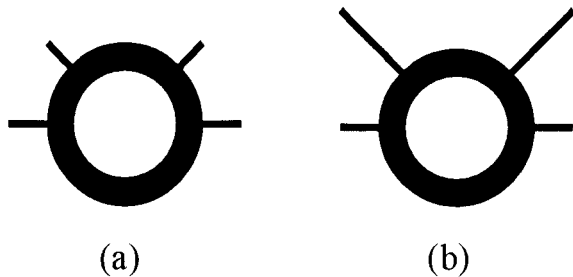


**Figure 3** (a) Conventional ring coupler; (b) modified ring coupler

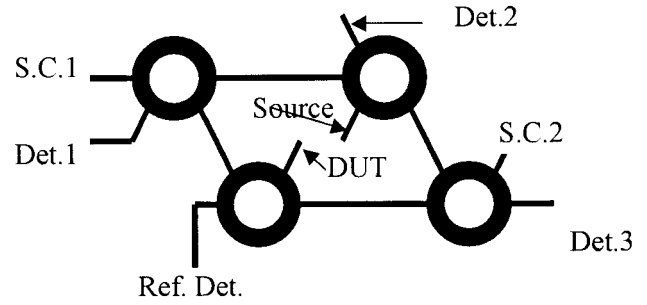


**Figure 4** Six-port reflectometer (construction 1)

modified ring couplers, short circuits (SCs), and (possibly) a matched load (ML). Also, in all these constructions, the ring couplers are separated from each other by  $\lambda/2$ , while the short circuits, matched load, and device under test (DUT) are  $\lambda/2$  away from the ring couplers. The power detectors are  $\lambda/4$  away from the ring couplers.

### 2.1. Construction 1

This construction consists of four ring couplers with two SC terminations, as shown in Figure 4. By using the transmission-line method, and after some mathematical manipulations, the power ratios at the measured ports are given by

$$P_1 = \frac{P_{Det.1}}{P_{Ref. Det.}} = \frac{(1 + \cos 2\theta)}{4(1 - \cos 2\theta)} \left| \Gamma_L - \frac{2e^{j4\theta}}{1 + e^{-j2\theta}} \right|^2, \quad (2.1)$$

$$P_2 = \frac{P_{Det.2}}{P_{Ref. Det.}} = \frac{(1 + \cos 2\theta)}{4} \left| \Gamma_L - \frac{2e^{j2\theta}}{1 + e^{-j2\theta}} \right|^2, \quad (2.2)$$

$$P_3 = \frac{P_{Det.3}}{P_{Ref. Det.}} = \frac{(1 + \cos 2\theta)}{4(1 - \cos 2\theta)} \left| \Gamma_L - \frac{2}{1 + e^{-j2\theta}} \right|^2. \quad (2.3)$$

Eng et al. [7] choose  $\theta = 60^\circ$  for such a construction, so that the locations of the  $q$  points are  $(-60^\circ, 180^\circ, 60^\circ)$  and the  $q$  values are equal ( $|q_1| = |q_2| = |q_3| = 2$ ). In fact, another solution was found by taking  $\theta = 45^\circ$ , so that the locations of the  $q$  points are  $(-135^\circ, +135^\circ, 45^\circ)$  and the  $q$  values are equal ( $|q_1| = |q_2| = |q_3| = \sqrt{2}$ ). The last solution has a smaller size than that in [7]; also, the positions of the  $q$  points are near to the origin, and hence the intersection of the three circles that represent the power ratios are improved.

### 2.2. Construction 2

This construction consists of four ring couplers with two SC terminations, while the DUT and source ports are outside the construction and thus easily can reach the feed source and connect to the DUT (see Fig. 5). By using the same procedure, the power equations are as follows:

$$P_1 = \frac{(1 + \cos 2\theta)}{4(1 - \cos 2\theta)} \left| \Gamma_L - \frac{2e^{j2\theta}}{1 + e^{-j2\theta}} \right|^2, \quad (3.1)$$

$$P_2 = \frac{(1 + \cos 2\theta)}{4} \left| \Gamma_L - \frac{2}{1 + e^{-j2\theta}} \right|^2, \quad (3.2)$$

$$P_3 = \frac{(1 + \cos 2\theta)}{4(1 - \cos 2\theta)} \left| \Gamma_L - \frac{2e^{-j2\theta}}{1 + e^{-j2\theta}} \right|^2. \quad (3.3)$$

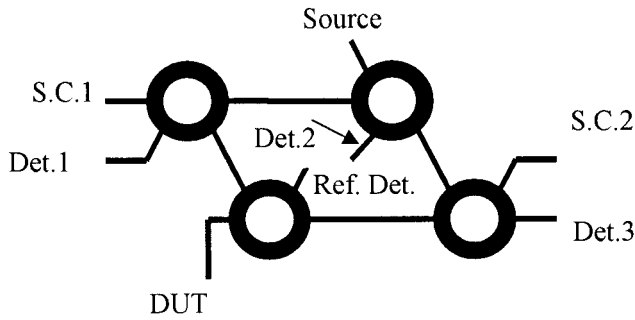


Figure 5 Six-port reflectometer (construction 2)

When choosing  $\theta = 45^\circ$ , the locations of the  $q$  points are  $(135^\circ, +45^\circ, -45^\circ)$  and the  $q$  values are equal ( $|q_1| = |q_2| = |q_3| = \sqrt{2}$ ). Also, when choosing  $\theta = 60^\circ$ , the locations of the  $q$  points are  $(180^\circ, 60^\circ, -60^\circ)$  and the  $q$  values are equal ( $|q_1| = |q_2| = |q_3| = 2$ ). Both solutions have equal  $q$  values and are uniformly distributed around the origin.

### 2.3. Construction 3

This construction is shown in Figure 6. It is clear that both the source and the DUT ports are outside the construction and only one detector is inside the construction. Similarly, the power relations will be as follows:

$$P_1 = \frac{(1 - \cos 2\theta)}{8} \left| \Gamma_L - \frac{e^{-j2\theta}(1 + e^{-j2\theta})}{e^{-j2\theta} - 1} \right|^2, \quad (4.1)$$

$$P_2 = \frac{1}{8} |\Gamma_L - e^{-j(2\theta \pm \pi)}|^2, \quad (4.2)$$

$$P_3 = \frac{(1 + \cos 2\theta)}{8} \left| \Gamma_L - \frac{e^{-j2\theta}(e^{-j2\theta} - 1)}{1 + e^{-j2\theta}} \right|^2. \quad (4.3)$$

When choosing  $\theta = 45^\circ$ , the locations of the  $q$  points are  $(0^\circ, 90^\circ, \text{and } 180^\circ)$  and the  $q$  values are equal ( $|q_1| = |q_2| = |q_3| = 1$ ). Also, when choosing  $\theta = 60^\circ$ , the locations of the  $q$  points are  $(-30^\circ, 60^\circ, 150^\circ)$ , but the  $q$  values are not equal ( $|q_1| = 0.577, |q_2| = 1, |q_3| = \sqrt{3}$ ). Both solutions are uniformly distributed around the origin, while only one of them has equal  $q$  values.

### 3. DESIGN AND SIMULATION

As an example, construction 3 (with  $\theta = 45^\circ$ ) is designed on an RT/Duroid 5880 ( $\epsilon_r = 2.2, H = 0.7874$  mm) at 3-GHz center frequency. The geometrical dimensions of the ring coupler are

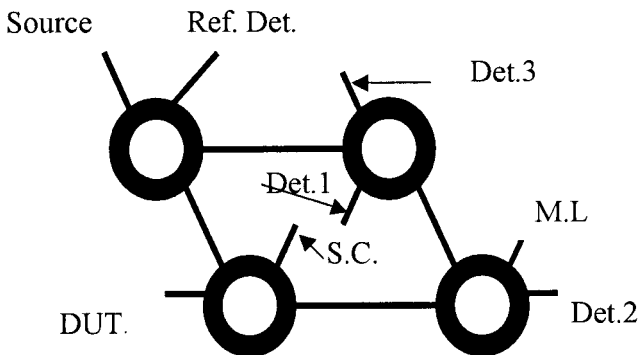


Figure 6 Six-port reflectometer (construction 3)

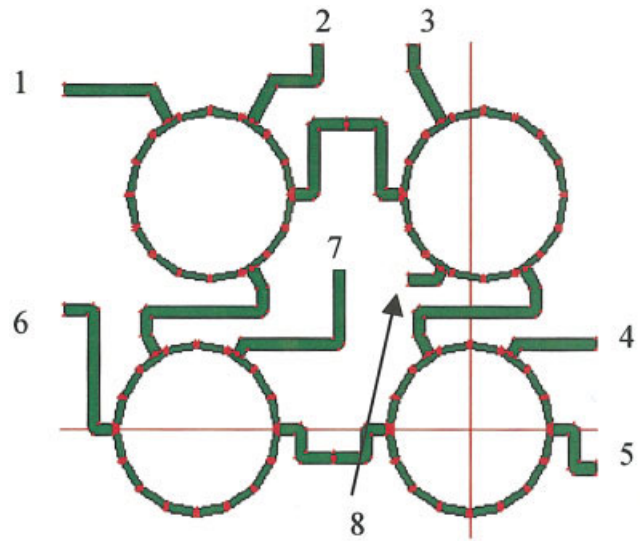


Figure 7 Realized six-port reflectometer [Color figure can be viewed in the online issue, which is available at [www.interscience.wiley.com](http://www.interscience.wiley.com).]

$W_{arms} = 2.4255$  mm  $W_{ring} = 1.3852$  mm, each ring's mean radius is 10.634 mm, and the interconnection line between the two rings is  $\lambda/2 = 36.552$  mm (see Fig. 7). First, an IE3D simulator (Zeland, Inc.) is used to simulate the six-port reflectometer (the  $S$  parameters are shown in Fig. 8), while the DUT port is connected to a perfectly matched load. From Figure 8, it is clear that there is a very good isolation between the DUT port and the reference detector port (this is one of the design objectives of the reflectometer system), so that the reading provided by the reference port will be proportional to the power incident on the DUT port [7].

### 4. CALIBRATION

The above equations (Eqs. 2, 3 and 4) can be rewritten in the form:

$$\begin{aligned} P_1 &= |A|^2 |\Gamma_L + B|^2 \\ P_2 &= |C|^2 |\Gamma_L + D|^2 \\ P_3 &= |E|^2 |\Gamma_L + F|^2. \end{aligned} \quad (5)$$

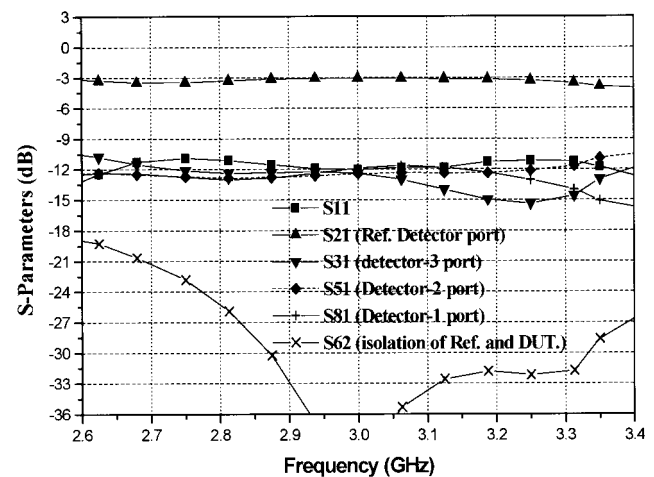


Figure 8 Simulated  $S$  parameters of the realized six-port reflectometer

**TABLE 1 Comparison Between Measurements of the Realized Six-Port Reflectometer and Vector Network Analyzer (Agilent 8719ES) at  $F = 3.0$  GHz**

Load Type	Six-Port Reflectometer	Vector Network Analyzer
Sliding load	$0.005213 < 120^\circ$	$0.005113 < 127.5^\circ$
Sliding short circuit	$0.982100 < 129^\circ$	$0.972105 < 131^\circ$
	$0.932710 < -16.57^\circ$	$0.9335160 < -15.0^\circ$
	$0.892357 < 29.65^\circ$	$0.910025 < 27.5^\circ$
	$0.965231 < -44.12^\circ$	$0.970251 < -45.2^\circ$
	$0.922518 < -145.3^\circ$	$0.935287 < -146.7^\circ$
	$0.91878 < 217.86^\circ$	$0.932850 < 220.12^\circ$

$P_1$ – $P_3$  are the power ratios, while  $A$ ,  $C$ , and  $E$  are three real calibration constants, and  $B$ ,  $D$  and  $F$  are three complex calibration constants, so there are nine unknowns. The purpose of the calibration is to calculate these unknowns (calibration constants). By using three positions of a sliding short circuit with a matched load (calibration procedure [4, 11]), the above unknowns are obtained. When an unknown impedance is connected to the DUT port, the power reading at the four detector ports will represent three circles in a complex  $\Gamma$ -plane. The intersection point of these three circles will give the reflection coefficient magnitude and phase (see Fig. 2). In fact, the intersection of the three circles in one point is theoretical, because real systems are not stable, so the related geometrical configurations never have a single intersection points. By considering the intersection region as a triangle, we have different solutions such as: the intersection point of the medians of the triangle, the intersection point of the perpendicular bisectors of the triangle sides, the intersection points of the bisectors of the triangle interior angles, the intersection point of the three altitudes of the triangle, and so on.

## 5. MEASUREMENT AND RESULTS

The above-realized six-port reflectometer was first calibrated in order to calculate the calibration constants. Then it was used to measure the reflection coefficient of different unknown impedances (especially different positions of sliding SCs) and good agreement with the measurements of the vector network analyzer (Agilent 8719ES), with error not exceeding 2.5% in magnitude and  $\pm 3^\circ$  in phase in the operating range 2.67–3.25 GHz, was obtained. Table 1 illustrates some measurements at the 3-GHz center frequency. A shift of 40 MHz in the center frequency was found, due to the mismatch of the intersection lines that connect the ring couplers to each other and some tolerance in fabrication.

In fact, the overall dimensions of the realized six-port reflectometer is around  $10 \times 10$  cm, which is very large. To reduce the size, we can use modified ring couplers [12], which are only 15% of the conventional ring coupler's size, and replace the intersection between couplers by its corresponding T or  $\Pi$  junctions [12]. Currently, some trials are being conducted in which no detectors are inside the construction and this design problem is under study.

## 6. CONCLUSION

A six-port reflectometer constructed from a  $0^\circ/180^\circ$  ring coupler has been presented. Three different constructions with their  $q$  positions are given. One of these constructions was realized on an RT/Duroid 5880 at 3-GHz center frequency. The realized six-port reflectometer was first calibrated and then used to measure the reflection coefficient of different unknown impedances. The six-port reflectometer was in good agreement with the measurements of the vector network analyzer (Agilent 8719ES), especially in the microwave range 2.67–3.25 GHz.

## ACKNOWLEDGMENT

The author would like to thank Prof. Esmat A.F. Abdallah, Electronics Research Institute, Egypt, for her useful discussions during the production of this work.

## REFERENCES

- G.F. Engen, The six-port reflectometer: An alternative network analyzer, *IEEE Trans Microwave Theory Tech* 25 (1977), 1075–1080.
- P. Groll and W. Khol, Six-port consisting of two directional couplers and two voltage probes for impedance measurement in the millimeter wave range, *IEEE Trans Instrum Meas* 29 (1980), 386–390.
- D. Pavaldis and H.L. Hartnagel, The design and performance of three-line microstrip coupler, *IEEE Trans Microwave Theory Tech* 24 (1976), 631–640.
- R.J. Collier and N.A. El-Deeb, Microstrip coupler suitable for use as a six-port reflectometer, *Proc IEE* 127 H (1980), 87–91.
- E.R. Hansson and G.P. Ribblet, An ideal six-port network consisting of a matched reciprocal lossless five port and a perfect directional coupler, *IEEE Trans Microwave Theory Tech* 31 (1983), 284–288.
- G.F. Engen, A historical review of the six-port measurement technique, *IEEE Trans Microwave Theory Tech* 45 (1997), 2414–2417.
- S.G. Eng, K.W. Eccleston, and S.P. Yeo, Re-designing six-port reflectometer based on four port coupler, *Int Symp Microwave Opt Technol*, Montreal, Canada, 2001, pp. 19–23.
- G.F. Engen, Determination of microwave phase and amplitude from power measurements, *IEEE Trans Instrum Meas* IM-25 (1976), 414–418.
- G.F. Engen, An improved circuit for implementing six-port technique of microwave measurements, *IEEE Trans Microwave Theory Tech* MTT-25 (1977), 1080–1083.
- H.M. Cronson and R.A. Fong-Tom, A 94-GHz diode based single six-port reflectometer, *IEEE Trans Microwave Theory Tech* MTT-30 (1982), 1260–1264.
- A.S. Mohra, Six-port reflectometer realization using two microstrip three-section couplers, *Proc 18<sup>th</sup> Natl Radio Sci NRSC2001*, Mansoura University, Egypt, 2001, pp. 27–29.
- A.S. Mohra, A.F. Sheta, and S.F. Mahmoud, A small size 3-dB  $0/180^\circ$  microstrip ring couplers, *J Electromagn Wave Appl* 17 (2003), 707–718.

© 2004 Wiley Periodicals, Inc.

## BENT PLANAR MONOPOLE OPERATING AT GSM/DCS/PCS/IMT2000 QUAD-BANDS

T. K. William Low,<sup>1,2</sup> Zhi Ning Chen,<sup>1</sup> and Ning Yang<sup>1</sup>

<sup>1</sup> Institute for Infocomm Research  
20 Science Park Road  
#02-34/37 Teletech Park  
Singapore 117674

<sup>2</sup> Department of Electrical and Computer Engineering  
National University of Singapore  
10 Kent Ridge Crescent  
Singapore 119260

Received 25 June 2003

**ABSTRACT:** In this paper, a compact antenna operating in the GSM/DCS/PCS/IMT2000 quad-bands is presented. By bending the meandered monopole into three equal and perpendicular sections, then coupling the bent monopole with another strip monopole antenna, the designed novel antenna covers the required bandwidths of GSM (890–960 MHz), DCS (1710–1880 MHz), PCS (1850–1990 MHz) and IMT2000 (1900–2025 MHz). © 2004 Wiley Periodicals, Inc. *Microwave Opt Technol Lett* 40: 170–172, 2004; Published online in Wiley InterScience (www.interscience.wiley.com). DOI 10.1002/mop.11319